Available online at www.sciencedirect.com
ScienceDirect
Journal of Magnetic Resonance 193 (2008) 1–9
JMR Journal of Magnetic Resonance
www.elsevier.com/locate/jmr

Magnetic resonance in systems with equivalent spin-1/2 nuclides. Part 2: Energy values and spin states

Sergiy M. Nokhrin, David F. Howarth, John A. Weil *

Departments of Chemistry and Geological Sciences, 110 Science Place, University of Saskatchewan, Saskatoon, SK, Canada S7N 5C9

Received 26 September 2007; revised 23 January 2008
Available online 15 February 2008

Abstract

In an earlier paper (Part 1), featuring group-theoretical analysis, it was shown that the isotropic EPR spectra of free radical ($S = 1/2$) species XL_n, where the n equivalent nuclei also have spin 1/2, have a more complicated form than anticipated from the usual (first-order) oversimplified analysis. The nucleus of X is taken to be spin-less. The latter predicts $n + 1$ lines with intensity ratios given by the coefficients of the binomial expansion; for systems with $n = 3$, the EPR spectrum in fact consists of 6 lines. Analogous considerations hold for NMR spectroscopy of XL_n non-radicals. For $n \geqslant 3$ systems, the degeneracy of the energy levels cannot be completely removed by the Zeeman electronic and nuclear interactions. Explicit solutions for $n = 3$ (analytic, as well as computational) of the spin-hamiltonian for the energies and spin states have been obtained and are given in the present work. Discussion of the underlying theory, invoking exchange degeneracy, is included herein in some detail, focusing on line positions and relative spectral intensities.

Keywords: EPR; NMR; Hyperfine; Equivalent nuclides; Spin-hamiltonian energies and eigenstates; Exchange degeneracy

1. Introduction

This paper is a continuation of the earlier one [1], in which we set out the problem, summarized the earlier literature, discussed various chemical examples (species XL_n in which the ligand nuclei each have spin 1/2), and presented a primarily group-theoretical analysis. The nucleus of X is taken to be spin-less. The problem is to quantify and understand the EPR spectra of free radical ($S = 1/2$) species XL_n, and NMR spectra of analogous non-radical molecules, partly in an attempt at clarification of common misunderstandings to be found in the literature.

2. General theory

We wish in this work to pay particular attention to the theory underlying the spin states of a system XL_n and their energies, for arbitrary values of ligand number n. It should be noted that herein the system of n magnetically equivalent nuclei, all with spin 1/2, will be treated. This means that all nuclei within a set L have the same values of hyperfine coupling parameters A and effective nuclear g-factors g_n. Such equivalence can arise naturally from the symmetry of the molecule or through effective symmetry achieved by rapid internal motion.

Once again placing special emphasis on $n = 3$, keeping in mind the relevant energy-level scheme $E(B)$ (Fig. 1, which has been repeated from Part 1 of this work = [1]) for XL_3, we note some special aspects of the underlying theory:

(1) There exist sets of energies which are degenerate, and which remain exactly superimposed for all applied magnetic-field values B.
(2) The B-independent degeneracy arises from the invariance of the spin-hamiltonian with respect to all sets of pairwise permutations of equivalent nuclei, i.e., it is the so-called 'exchange degeneracy' ([2], p. 391). It is absent for $n = 1$ and 2.The spin-hamiltonian matrix for XL_3 can be factored so that exact energy expressions are available (Appendix A).

* Corresponding author. Fax: +1 306 966 4730.
E-mail address: john.weil@usask.ca (J.A. Weil).

1090-7807/$ - see front matter © 2008 Elsevier Inc. All rights reserved.
doi:10.1016/j.jmr.2008.02.010

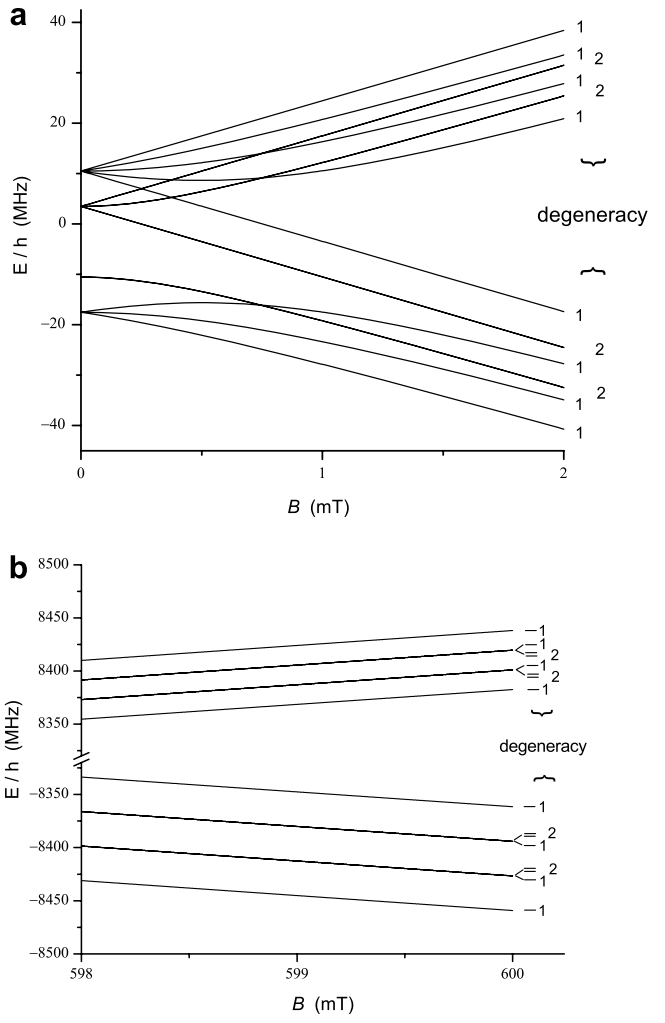

Fig. 1. The Zeeman energy-level diagram, for the hypothetical isotropic species XH_3 having one unpaired electron ($g = 2.0030$) and three equivalent $I = 1/2$ nuclides, created using spin-hamiltonian [1] without nuclear exchange terms, and g_n for bare nucleus ^{1}H. Hyperfine parameter $A/(g_e\beta_e)$ was taken to be +0.500 mT ($A/h = 14.0$ MHz). (a) B from 0 to 2 mT. The field-independent degeneracies are listed at the right. The appropriate labels for the states at $B = 0$ are, in order of increasing energy: $F = 1, 0, 1, 2$. (b) $598 \leqslant B \leqslant 600$ mT. This shows the relative bunching of the upper octet of states as compared to the lower octet. At still higher fields, the two sets become more equally spaced.

The spin-hamiltonian operator for the XL_n system with one unpaired electron with spin $S = 1/2$ and n equivalent nuclei having spin $I = 1/2$ is given ([3], pp. 121,160; [4]) by

$$^{op}H_s = {}^{op}H^B + {}^{op}H^{hf} + {}^{op}H^{n,ss}(X,L) \quad (1a)$$

$$= \left(g\beta_e \mathbf{B}^T \cdot {}^{op}\mathbf{S} - g_n\beta_n \mathbf{B}^T \cdot \sum_{i=1,n} {}^{op}\mathbf{I}_i\right) + A\ {}^{op}\mathbf{S}^T \cdot \sum_i {}^{op}\mathbf{I}_i + \sum_{i<j} \mathbf{J}_{ij}\, {}^{op}\mathbf{I}_i^T \cdot {}^{op}\mathbf{I}_j \quad (1b)$$

Here the symbol n stands for 'nuclear', or else the total number of equivalent nuclei per molecule. The operator $^{op}H^B$ represents the Zeeman interactions of the electron and also of the nuclear spins, respectively, with the external magnetic field $\mathbf{B} \parallel \mathbf{z}$, $^{op}H^{hf}$ describes the isotropic hyperfine coupling between the electron and the nuclear spins, and $^{op}H^{n,ss}(X,L)$ describes the nuclear spin–spin interactions (to be neglected). Superscript T in Eq. (1b) denotes spatial matrix transposition.

The nuclear spin–spin coupling parameters are expected to be much smaller than the electron-spin–nuclear-spin (hyperfine) coupling parameters. Though such interactions are present, they will not affect the EPR spectrum of any XL_n system. Generally, the operator for the nuclear spin–spin interaction can be divided into two types: the coupling between non-equivalent nuclei $^{op}H^{n,ss}(X,L)$ (for cases when X also has non-zero nuclear spin) and that between the equivalent nuclei described by $^{op}H^{n,ss}(L)$. EPR transitions will be allowed only between states that have the same eigenvalue of the latter operator, to good approximation. Thus these coupling interactions basically have 'no' EPR spectroscopic effect.

The analogous problem has been considered in detail in NMR spectroscopy ([5], Ch. 6, pp.103–164; [6], pp. 172–258), where it is widely known that the spectrum of a system of nuclear spins that include a set of magnetically equivalent nuclei is independent of the spin coupling between nuclei within that set. A proof of this statement is available [7].

Similar considerations can be applied here for EPR. To good approximation, the EPR transitions are allowed only between states that give non-zero matrix elements of the EPR transition-moment operator $^{op}\mu_x$ (excitation magnetic field along $\mathbf{x}$). Since the operators of the nuclear spin–spin interactions commute with the electron spin operator $^{op}S_x$, i.e., $[^{op}H^{n,ss}(X,L),\ ^{op}S_x] = 0$, the matrix element $(^{op}\mu_x)_{pq} \neq 0$ for any two states ϕ_p and ϕ_q only when $(^{op}H^{n,ss})_p = (^{op}H^{n,ss})_q$. Therefore there is no change in the energy of nuclear spin–spin interaction during an allowed EPR transition, and such an interaction does not affect the EPR spectrum of the XL_n system. So, the last term in spin-hamiltonian (Eqs. (1)) can usually be omitted, which simplifies further the consideration of such systems.

If the system contains n equivalent nuclei, all having spin $I = 1/2$, there will be a total of 2^n possible nuclear–spin eigenstates. Calculation of the energies and the eigenstates of spin-hamiltonian (Eqs. (1)) is feasible if the representation is chosen such that the nuclear spins occur coupled to form total nuclear spin $\sum_i \mathbf{I}_i$. In [8], it was shown that such a representation allows calculation of the EPR spectrum of a system with a set of n equivalent nuclei without explicit consideration of the 2^n nuclear-spin functions and, utilizing second-order perturbation theory for the hyperfine interactions, some features of the experimentally observed EPR spectra were explained. However, for explanation of many of the peculiarities of the EPR spectra of such systems, exact solution of spin-hamiltonian (Eqs. (1)) is desirable and, as discussed in Part 1 [1], this problem can be solved exactly for any n.

In the XL_n systems of interest herein, there are $(2S+1)(2I+1)^n$ spin states. The spin-hamiltonian operator matrix will have dimension $d \equiv 2^{n+1} \times 2^{n+1}$. Matrix

H^B will have only diagonal elements, whereas H^{hf} may have non-zero off-diagonal elements. The solutions of the corresponding secular equation are the energy levels, and the correct state 'functions' are the linear combinations of the basic product 'functions' (bras and kets Ψ), which diagonalize H_s. The secular equation can be factored into equations of order lower than d if we utilize the basic product functions classified according to the values of the total spin angular momentum projection quantum number F_z (alias M_F, the projection being along the total spin direction $\mathbf{z}_F$) and by choosing as basis functions linear combinations of product kets that transform according to the appropriate symmetry group. All the basic 'functions' are eigenkets of operator ${}^{op}F_z$, and each corresponds to a definite value of F_z. This classification allows one to simplify the secular equation since there are no off-diagonal elements of the spin-hamiltonian [1] between basic product kets that correspond to different values of F_z. The latter statement can be proved: Taking $|\Psi_i\rangle$ and $|\Psi_j\rangle$ as basic product kets that correspond to different values of F_z, one has:

$$\langle\Psi_i|H_sF_z|\Psi_j\rangle = (F_z)_j\langle\Psi_i|H_s|\Psi_j\rangle, \tag{2a}$$

$$\langle\Psi_i|F_zH_s|\Psi_j\rangle = (F_z)_i\langle\Psi_i|H_s|\Psi_j\rangle. \tag{2b}$$

Since ${}^{op}F_z$ commutes with ${}^{op}H^{hf}$ and consequently with the total spin-hamiltonian ${}^{op}H_s$, the left-hand side of these equations must be equal, so it follows that $\langle\Psi_i|H_s|\Psi_j\rangle = 0$, when $(F_z)_i \neq (F_z)_j$. This is also easily demonstrated using group theory.

The spin-hamiltonian for the XL_n system must remain unchanged under any permutation of equivalent nuclei. Then each of the individual state functions or sets of degenerate functions must transform in the same way, as one of the symmetry species (irreducible representations) of the appropriate permutation group. Hence states which belong to different symmetry species cannot 'interact' with one another.

To build appropriate state functions, we first can consider the nuclear spin parts alone, as follows.

We have seen in Part 1 of this work [1] that, for XL_3, the three product functions with $M_I = +1/2$ can be combined to give one linear combination in the completely symmetric species A_1 and one degenerate pair in species E. The actual linear combinations can be constructed using the formula

$$\Psi^\alpha = \eta \sum_{P=1,\ldots,n_p} \chi^\alpha_P \, P \, {}^{+1/2}\Psi(0) \tag{3}$$

([9], pp. 111–113; [10], p. 336), where the sum goes over all the operations of the permutation group at hand ($n_p = 6$ for XL_3). Here Ψ^α is the desired symmetry combination of the species, η is the normalizing factor, and χ^α_P is the character for the particular permutation P of the symmetry species. The generator function ${}^{+1/2}\Psi(0)$ is any one appropriate nuclear product ket. Here the pre-superscript is the total M_I. Thus, utilizing XL_3 as example, one has:

(a) Taking ${}^{+1/2}\Psi(0) \equiv |-++\rangle$, we obtain the Ψ^α combinations for $M_I = +1/2$:

$${}^{+1/2}|A_1\rangle = (1/\sqrt{3})(|++-\rangle + |+-+\rangle + |-++\rangle), \tag{4a}$$

$${}^{+1/2}|E_1\rangle = (1/\sqrt{6})(|++-\rangle + |+-+\rangle - 2|-++\rangle). \tag{4b}$$

To obtain the state function:

$${}^{+1/2}|E_2\rangle = (1/\sqrt{2})(|++-\rangle - |+-+\rangle), \tag{4c}$$

one can use the product function $|+-+\rangle$ as ${}^{+1/2}\Psi(0)$.

(b) The nuclear spin state functions for $M_I = -1/2$ can be obtained in complete analogy with the above derivation of the functions for $M_I = +1/2$, and one arrives at:

$${}^{-1/2}|A_1\rangle = (1/\sqrt{3})(|+--\rangle + |-+-\rangle + |--+\rangle), \tag{5a}$$

$${}^{-1/2}|E_1\rangle = (1/\sqrt{6})(2|+--\rangle - |-+-\rangle - |--+\rangle), \tag{5b}$$

$${}^{-1/2}|E_2\rangle = (1/\sqrt{2})(|-+-\rangle - |--+\rangle). \tag{5c}$$

(c) For $M_I = +3/2$, there is only one function:

$${}^{+3/2}|A_1\rangle = |+++\rangle. \tag{6}$$

(d) For $M_I = -3/2$, there again is only one function:

$${}^{-3/2}|A_1\rangle = |---\rangle. \tag{7}$$

Finally, to obtain the total spin product state functions of the system, one must supply the electron spin part for these functions, taken simply as products.

The spin-hamiltonian matrix expressed in this basis is seen to have a particularly simple form, since non-zero matrix elements occur only between:

(a) states with the same eigenvalue F_z. The latter remains a good quantum number at all fields B;
(b) states which belong to the same symmetry representation. Note that when state functions are members of a degenerate (E) set but are orthogonal, the matrix element of ${}^{op}H_s$ between them will be zero.

The spin-hamiltonian matrix for system XL_3 with these properly chosen functions, as shown in Appendix A, is factored into 1×1 and 2×2 matrices, and hence this problem can be easily solved exactly. The energy levels and eigenstates are given in Appendix A. Since operators ${}^{op}F^2$, ${}^{op}F_z$, and all permutation operators commute with spin-hamiltonian operator ${}^{op}H_s$ the state kets (or bras) can be chosen to be simultaneous eigenkets of all these operators, and these 'functions' are classified (see Appendix A) by quantum numbers F, F_z and according to the irreducible representation of the symmetry group to which they belong.

For simplicity, we shall focus in what follows on transitions in which $|\Delta F_z| = 1$ and in which the nuclei don't flip relative to each other (i.e., no difference in the irreducible representations of the two states involved). We'll deal primarily with EPR, and shall herein ignore all mixed EPR–NMR transitions (transitions with $\Delta M_S = \pm 1$, $\Delta M_I \neq 0$). Also, we shall not explicitly deal with pure NMR spectra.

Let us consider the transition energies and relative intensities of the EPR spectra of the XL_3 system. As was already mentioned, the magnetic dipole transitions are allowed only between states, which give non-zero matrix elements of the (electronic & nuclear) transition-moment operator

$$^{op}\mu_x = g\beta_e\,^{op}S_x - g_n\beta_n\Sigma_i\,^{op}I_{xi}.$$

The magnetic excitation is taken herein with field $\mathbf{B}_1$ to be $\perp \mathbf{B}$, but the details will not be discussed [Consult [3]; Program EPR–NMR [11] does evaluate these elements]. The non-zero matrix elements of $^{op}\mu_x$ occur only between states which belong to the same symmetry and for which $\Delta M_F = \pm 1$, (these two statements are the selection rules for the magnetic dipole transitions for such systems). For pure EPR, this becomes $\Delta M_S = \pm 1$.

It will prove convenient for analysis of the combination kets and the relative intensities to define, in Appendix A, a set of 4 auxiliary angles $\xi = \delta_1, \delta_2, \eta_1, \eta_2$, which is useful in writing the mixing coefficients. We also define convenient parameters $Y \equiv g\beta_e B/2$, and $Z \equiv g_n\beta_n B/2$. All 4 angles are specified by parameters $= A$, Y and Z, and thus are interrelated. At the limit $B = 0$, $\tan(2\delta_1) = -\tan(2\delta_2) = \pm 3^{1/2}$, $\tan(2\eta_1)$ and $\tan(2\eta_2) = \pm\infty$; furthermore, as $B \to \infty$, $\tan(2\xi) \to 0$.

At $B = 0$, the energy levels occur at $3A/4$, $A/4$, $-3A/4$ and $-5A/4$. The situation for $A > 0$ is shown for XH_3 in Fig. 1a. The diagram obviously becomes upside-down for $A < 0$, but no spectral changes will occur in that case. At higher B fields, with $A > 0$, the upper octet of states tends to bunch as compared to the lower one (see Fig. 1b), as a result of the respective destructive and constructive interference effects of the hyperfine and nuclear Zeeman terms.

Using the calculated eigenenergies and eigenstates for the XL_3 system, the EPR transition energies and relative intensities can be calculated. All the transitions considered herein occur between irreducible nuclear representations identical for both states involved. Details of the usual 8 main EPR transitions are presented in Table 1. However, as will be shown below, not only the line positions but also the number of resonance lines will be quite different at different ratios between the magnitude of the hyperfine coupling A and the Zeeman energy. We can discuss distinct cases.

Table 1 shows that, at $B = 0$, all 8 'main' EPR transitions vanish in intensity. However, we see from Table 2 that here there are 8 other transitions with non-zero intensity factors. Fig. 2 presents a frequency-swept spectrum depicting this situation.

We consider next the case of the strong B-field, sufficiently so that the Zeeman electron energy and thus the required photon energy is much larger than the hyperfine interaction: $h\nu \gg |A|$ and $|A| \gg |Z|$, which is a common case. This field is to be greater than any field at which an energy-level crossing occurs. This has been until now the usual experimental case. Note the energy-level diagram of the XL_3 system (Figs 1a and 1b, and Fig. 2 of Part 1 = [1] of this work). The spin states, labeled *1, …, 16* in descending energy order (see Appendix B), in the high B-field region as defined above, and with $Y \gg Z > 0$, are:

Table 1
The six distinct sets[a] of major transitions for fixed-frequency $|\Delta F_z| = 1$ EPR [see Fig. 2 of Part 1], of an $S = 1/2$ molecular species XL_3, listed in the order of increasing transition energies @ fixed magnetic field (i.e., decreasing resonance fields B @ fixed frequency), including the relative intensity factors arising from the mixing coefficients

Transition[b,c]	Transition energy ΔE	Intensity factor[d,e]
$\phi_1 \leftrightarrow \phi_9$ $\|2, -1, A_1\rangle \leftrightarrow \|2, -2, A_1\rangle$	$Y - A + \{(Y + Z - A/2)^2 + (3/4)A^2\}^{1/2} - Z$	$\cos\delta_2$
$\phi_{3,4} \leftrightarrow \phi_{10,11}$ $\|1, 0, E_{1,2}\rangle \leftrightarrow \|1, -1, E_{1,2}\rangle$	$Y - A/2 + \{(Y + Z)^2 + (A/2)^2\}^{1/2} - Z$	$\sqrt{2}\cos\eta_2$
$\phi_2 \leftrightarrow \phi_{12}$ $\|2, 0, A_1\rangle \leftrightarrow \|1, -1, A_1\rangle$	$\{(Y + Z)^2 + A^2\}^{1/2} + \{(Y + Z - A/2)^2 + (3/4)A^2\}^{1/2} - 2Z$	$\cos\delta_2\cos\eta_1$
$\phi_{6,7} \leftrightarrow \phi_{13,14}$ $\|1, +1, E_{1,2}\rangle \leftrightarrow \|0, 0, E_{1,2}\rangle$	$Y + A/2 + \{(Y + Z)^2 + (A/2)^2\}^{1/2} - Z$	$\sqrt{2}\cos\eta_2$
$\phi_5 \leftrightarrow \phi_{15}$ $\|2, +1, A_1\rangle \leftrightarrow \|1, 0, A_1\rangle$	$\{(Y + Z)^2 + A^2\}^{1/2} + \{(Y + Z + A/2)^2 + (3/4)A^2\}^{1/2} - 2Z$	$\cos\delta_1\cos\eta_1$
$\phi_8 \leftrightarrow \phi_{16}$ $\|2, +2, A_1\rangle \leftrightarrow \|1, +1, A_1\rangle$	$Y + A + \{(Y + Z + A/2)^2 + (3/4)A^2\}^{1/2} - Z$	$\cos\delta_1$

The 16 energy eigenkets ϕ_i are defined in Appendix A, and $Y \equiv g\beta_e B/2$, $Z \equiv g_n\beta_n B/2$. Angles δ_1, δ_2, η_1, η_2 occurring in column 3 are defined in Appendix A, and are functions of A, Y and Z.

[a] The kets in column 1 are labeled with: zero-field F, M_F, irreducible representation of permutation group P_3. Notation $\phi_{a,b} \leftrightarrow \phi_{c,d}$ denotes 2 transitions. All square-root quantities $\{\}^{1/2}$ are to be taken as non-negative.

[b] The labels on kets ϕ_j ($j = 1, 2, \ldots, 16$) refer to the states in the highest B-field region, $j = 1$–8 denoting the states with positive energy, and $j = 9$–16 to the negative-energy states (when $Y \gg Z > 0$).

[c] Note the different meanings within the set of symbols A_1, as well as of E_1 and E_2, in the two kets given in column 1: see Appendix A. Thus the 1st column 1st row item should actually read $|2, -1, A_1^{iv}\rangle \leftrightarrow |2, -2, {}^{-3/2}A_1\rangle$.

[d] The factor $\sqrt{2}$ in the 3rd column indicates that there are two degenerate transitions superimposed.

[e] For the angle set $\xi = \delta_1, \delta_2, \eta_1, \eta_2$: At $B = 0$, $\pm\cos(\xi)$ is $3^{1/2}/2$, $1/2$, $1/2^{1/2}$, $1/2^{1/2}$, while $\sin(\xi)$ is $1/2$, $3^{1/2}/2$, $1/2^{1/2}$, $1/2^{1/2}$. In the limit as $B \to \infty$, $\cos(\xi) = 1$, $\sin(\xi) = 0$.

1	$\|2, -1, A_1\rangle$	*5*	$\|1, +1, E_2\rangle$	*9*	$\|2, -2, A_1\rangle$
2	$\|2, 0, A_1\rangle$	*6*	$\|1, +1, E_1\rangle$	*10*	$\|1, -1, E_1\rangle$
3	$\|1, 0, E_1\rangle$	*7*	$\|2, +1, A_1\rangle$	*11*	$\|1, -1, E_2\rangle$
4	$\|1, 0, E_2\rangle$	*8*	$\|2, +2, A_1\rangle$	*12*	$\|1, -1, A_1\rangle$
				13	$\|0, 0, E_1\rangle$
				14	$\|0, 0, E_2\rangle$
				15	$\|1, 0, A_1\rangle$
				16	$\|1, +1, A_1\rangle$.

The kets in the 2nd columns of the kets are labeled with: zero-field F, M_F, and the symbol for the irreducible representation of the permutation group P_3. Of course, there are actually eight representations A_1, which must be kept distinct for our purposes, say by labeling with superscripts i, ii, ..., as defined in Appendix A. Similarly, E_1 and E_2 need labeling into distinct pairs. With opposite signs of Y and Z, the energy ordering differs.

Calculated transition energies and relative intensities for the main EPR lines are given in Table 1. All these transitions go to maximum intensity factors as $B \to \infty$ (unity when A is finite). The theory shows that the EPR spectrum consists of 8 transitions, and can exhibit 6 distinct lines instead of only 4 lines with intensity ratios 1:3:3:1 as usually described. It follows from the results given in Table 1 that the splitting into line pairs (and each intensity factor) is strongly dependent on the ratio between the magnitude of the hyperfine coupling and the Zeeman energy.

In the region of increasingly strong applied magnetic fields B, this splitting into pairs can be approximated with the value $7A^2/(4g\beta_e B)$, and hence such splitting may be observed when either the hyperfine coupling is sufficiently large and/or the magnetic field is relatively small. For example, this splitting was experimentally observed in the EPR spectrum of the CF_3 radical ($g = 2.0032$) [12], for which the isotropic hyperfine coupling $A/(g_e\beta_e) = 14.05$ mT is large enough to observe such splitting even at X-band. As shown in Fig. 3 (also Fig. 2 of [12]), there are 2 pairs of lines spanning the middle instead of 2 equally intense lines. However, in many cases, the hyperfine coupling A is not large enough or when spectrum is measured at higher frequency, this splitting is not usually resolved, but shows up as affecting the effective relative intensities of the EPR peaks (see Fig. 4). As one can see from Table 1, the relative intensities of these lines are also dependent on the ratio $|A|/(h\nu)$ and are more sensitive to this ratio

Table 2
The 10 distinct sets[a] of fixed-frequency $|\Delta F_z| = 1$ transitions [other than the major EPR transitions listed in Table 1] of an $S = 1/2$ molecular species XL_3, including the relative intensity factors arising from the mixing coefficients

No.	Transition[b,c]	Transition energy ΔE	Intensity factor[d,e]
(1)	$\phi_5 \leftrightarrow \phi_8$ $\|2, +1, A_1\rangle \leftrightarrow \|2, +2, A_1\rangle$	$-Y - A + \{(Y+Z+A/2)^2 + (3/4)A^2\}^{1/2} + Z$	$\sin\delta_1$
(2)	$\phi_2 \leftrightarrow \phi_5$ $\|2, 0, A_1\rangle \leftrightarrow \|2, +1, A_1\rangle$	$\{(Y+Z)^2 + A^2\}^{1/2} - \{(Y+Z+A/2)^2 + (3/4)A^2\}^{1/2} + 2Z$	$\cos\delta_1 \sin\eta_1$
(3)	$\phi_1 \leftrightarrow \phi_2$ $\|2, -1, A_1\rangle \leftrightarrow \|2, 0, A_1\rangle$	$\{(Y+Z)^2 + A^2\}^{1/2} + \{(Y+Z-A/2)^2 + (3/4)A^2\}^{1/2} + 2Z$	$\sin\delta_2 \cos\eta_1$
(4)	$\phi_{3,4} \leftrightarrow \phi_{6,7}$ $\|1, 0, E_{1,2}\rangle \leftrightarrow \|1, +1, E_{1,2}\rangle$	$-Y + A/2 + \{(Y+Z)^2 + (A/2)^2\}^{1/2} + 2Z$	$-\sqrt{2}\sin\eta_2$
(5)	$\phi_{12} \leftrightarrow \phi_{15}$ $\|1, -1, A_1\rangle \leftrightarrow \|1, 0, A_1\rangle$	$\{(Y+Z)^2 + A^2\}^{1/2} - \{(Y+Z-A/2)^2 + (3/4)A^2\}^{1/2} + 2Z$	$-\cos\delta_2 \sin\eta_1$
(6)	$\phi_{15} \leftrightarrow \phi_{16}$ $\|1, 0, A_1\rangle \leftrightarrow \|1, +1, A_1\rangle$	$-\{(Y+Z)^2 + A^2\}^{1/2} + \{(Y+Z-A/2)^2 + (3/4)A^2\}^{1/2} + 2Z$	$-\sin\delta_1 \cos\eta_1$
(7)	$\phi_{10,11} \leftrightarrow \phi_{13,14}$ $\|1, -1, E_{1,2}\rangle \leftrightarrow \|0, 0, E_{1,2}\rangle$	$-Y + A/2 + \{(Y+Z)^2 + (A/2)^2\}^{1/2} + Z$	$\sqrt{2}\sin\eta_2$
(8)	$\phi_9 \leftrightarrow \phi_{12}$ $\|2, -2, A_1\rangle \leftrightarrow \|1, -1, A_1\rangle$	$-Y + A + \{(Y+Z-A/2)^2 + (3/4)A^2\}^{1/2} + Z$	$-\sin\delta_2$
(9)	$\phi_1 \leftrightarrow \phi_{15}$ $\|2, -1, A_1\rangle \leftrightarrow \|1, 0, A_1\rangle$	$-\{(Y+Z)^2 + A^2\}^{1/2} + \{(Y+Z+A/2)^2 + (3/4)A^2\}^{1/2} + 2Z$	$-\sin\delta_2 \sin\eta_1$
(10)	$\phi_2 \leftrightarrow \phi_{16}$ $\|2, 0, A_1\rangle \leftrightarrow \|1, +1, A_1\rangle$	$-\{(Y+Z)^2 + A^2\}^{1/2} + \{(Y+Z+A/2)^2 + (3/4)A^2\}^{1/2} + 2Z$	$-\sin\delta_1 \sin\eta_1$

The 16 energy eigenkets ϕ_i are defined in Appendix A, and $Y \equiv g\beta_e B/2$, $Z \equiv g_n\beta_n B/2$. Angles δ_1, δ_2, η_1, η_2 occurring in column 3 are defined in Appendix A, and are functions of A, Y and Z.

[a] The kets in column 1 are labeled with: zero-field F, M_F, irreducible representation of permutation group P_3. Notation $\phi_{a,b} \leftrightarrow \phi_{c,d}$ implies 2 transitions. All square-root quantities $\{\}^{1/2}$ are to be taken as non-negative.

[b] The labels on kets ϕ_j ($j = 1, 2, \ldots, 16$) refer to the states in the highest B-field region, $j = 1$–8 denoting the states with positive energy, and $j = 9$–16 to the negative-energy states (when $Y \gg Z > 0$).

[c] Note the different meanings within the set of symbols A_1, as well as of E_1 and E_2, in the two kets given in column 1: see Appendix A.

[d] The factor $\sqrt{2}$ in the 3rd column indicates that there are two degenerate transitions, superimposed.

[e] For the angle set $\xi = \delta_1, \delta_2, \eta_1, \eta_2$: At $B = 0$, $\pm\cos(\xi)$ is $3^{1/2}/2$, $1/2$, $1/2^{1/2}$, $1/2^{1/2}$, while $\sin(\xi)$ is $1/2$, $3^{1/2}/2$, $1/2^{1/2}$, $1/2^{1/2}$. In the limit as $B \to \infty$, $\cos(\xi) = 1$, $\sin(\xi) = 0$.

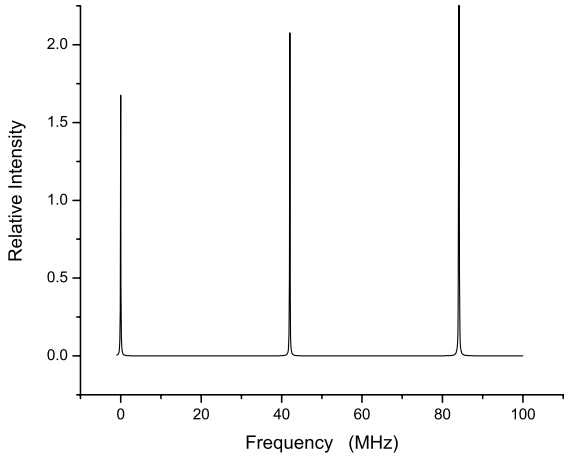

Fig. 2. The frequency-swept EPR spectrum, for a molecular group XF_3, as produced by computer program EPR–NMR [11], for zero external magnetic field B. The parameter $A/h = 42.0$ MHz ($A/(g_e\beta_e) = +1.500$ mT) was utilized, with individual lines taken to be lorentzians each with full width at half-height of 0.10 MHz. The three major lines, occurring at 0, A/h and 2 A/h, are of course multiply degenerate (see Tables 1 and 2).

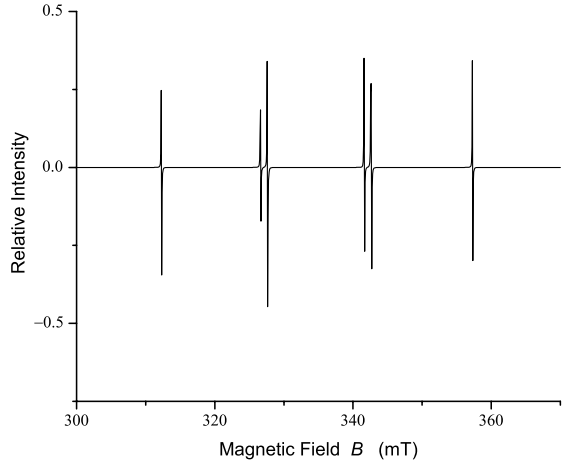

Fig. 3. The first-derivative field-swept EPR spectrum, for a molecular group XF_3, as produced by computer program EPR–NMR [11], for frequency 9.40 GHz (X-Band). The parameters $g = 2.0030$ and $A/(g_e\beta_e) = +15.0$ mT (large!) were utilized, with individual lines taken to be lorentzians each with max–min width of 0.050 mT.

than the splitting into pairs. Further work on the frequency dependence of the intensities of the various lines appearing in the field-swept spectra is being undertaken by us.

It is worthwhile to notice that various energy-level crossings occur when the Zeeman electronic energy $g\beta_e B \sim |A|/2$ (for example, see Fig. 1a at $B \sim 0.3$ mT). One can of course solve for the crossing fields $B_x(A)$ by setting up equalities between the appropriate energy relations found in Tables 1 and 2. The energy levels that become coincident belong to different symmetry species; there are no anti-crossings of levels. The crossings do not affect the spectra themselves.

An EPR spectrum for a molecular species XH_3, with $A/(g_e\beta_e) = 0.5$ mT (a typical value), simulated for the relatively low excitation frequency of 10.0 MHz, shows that only two lines (Fig. 5) with appreciable intensity are predicted, both occurring in the energy-level crossing region.

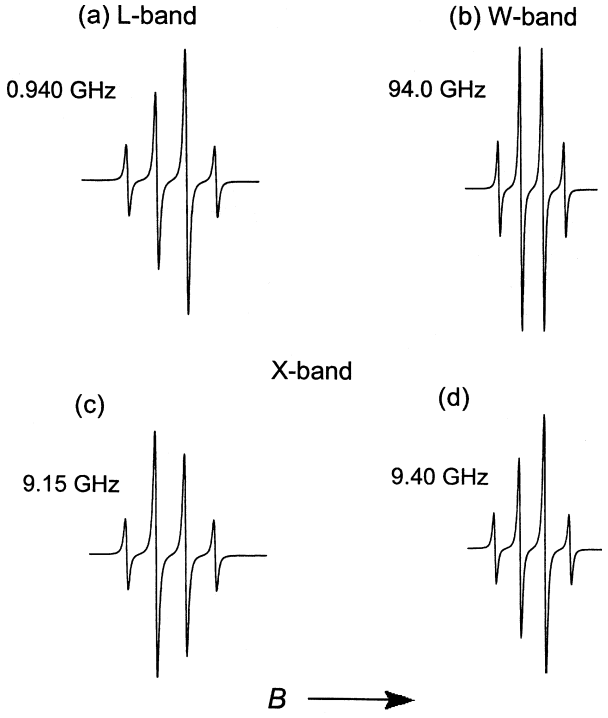

Fig. 4. The first-derivative field-swept EPR spectra, for a species XH_3, as produced by computer program EPR–NMR [11], for various frequencies (in GHz): (a) 0.940 (L-Band), (b) 94.0 (W-Band), (c) 9.15 (X-Band), and (d) 9.40 (X-Band). The parameters $g = 2.0030$ and $A/(g_e\beta_e) = +0.500$ mT were utilized, with individual lines taken to be lorentzians each with max–min width of 0.050 mT. The transitions at X-band, listed in order of increasing B field, are: *8–16*, *5–15*, (*6*, *7–13*, *14*), *2–12*, (*3*, *4–10*, *11*), *1–9*. Note the subtle intrinsic effects (which are real!) affecting the inner lines: compare X-band spectra (c) and (d).

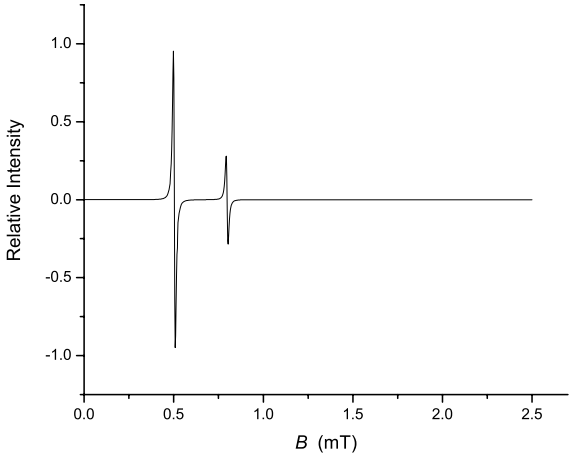

Fig. 5. The first-derivative field-swept EPR spectrum, for a species XH_3, as produced by computer program EPR–NMR [11], for the 'low' frequency 10.0 MHz. The parameters $g = 2.0030$ and $A/(g_e\beta_e) = +0.500$ mT were utilized, with individual lines taken to be lorentzians each with max–min width of 0.20 mT. The two EPR lines visible, appearing at 0.5038 (4-fold degenerate: {*3*, *4* ⇔ *10*, *11*}) and at 0.7982 mT {*8* ↔ *9*} [high-field state labels] are the only ones that match the available energy spacings (as per Fig. 1a), and have appreciable intensity.

The same situation is true with $A/(g_e\beta_e) = 5.0$ mT at 100 MHz, except that the two lines occur at fields higher by a factor of 10 and with greater intensity.

Note from the present theory that there also are 12 pure $|\Delta F_z| = 1$ transitions that vanish in intensity when field $B \to \infty$, as listed in Table 2. These transitions considered "forbidden" in the high magnetic-field region, where states can be characterized by M_S and M_I with high accuracy, appear as result of strong admixture of states with different (M_S, M_I) due to the off-diagonal terms in the spin-hamiltonian. So these transitions are expected to occur in the low magnetic-field region, where the electronic Zeeman energy has values of the same magnitude as that of hyperfine interaction ($g\beta_e B \sim |A|$).

Hence Tables 1 and 2 indicate that there are at most $8 + 12 = 20$ transitions of the type $|\Delta F_z| = 1$, which can in principle be observed. Note that transitions (1)–(6) in Table 2 can be observed only when transition energy $h\nu$ is smaller than ca. $|A|/2$. Such an energy quantum is sufficient to induce all transitions with $\Delta F = 0$ and $|\Delta F_z| = 1$; these are (1)–(6) from Table 2, transitions $\varphi_8 \leftrightarrow \varphi_9$ and $\varphi_{3,4} \leftrightarrow \varphi_{10,11}$ (see Fig. 5) listed in Table 1. Transitions (8) and (10) in Table 2 can be observed when $h\nu$ is larger than $2|A|$, and transitions (7) and (9) can be observed when $h\nu$ is smaller than $|A|$, but larger than ca. $|A|/2$. These transitions are very weak NMR transitions arising via the mixing of the two M_S states within some of the spin kets (see next paper in the present series).

The smallest transition energy required for 5 of these transitions is $2|A|$, as may be deduced from Table 1. Then, in the energy range $|A| < h\nu < 2|A|$, the energy quantum is not sufficient to induce all the pure EPR transitions, despite their non-zero intensity factors. In this case, only the 3 out of the 8 transitions described above for the strong-field case will be observable (Fig. 5). Similar considerations hold for the other $|\Delta F_z| = 1$ transitions, listed in Table 2. For the latter, most of the transitions feature appreciable dependence on the nuclear Zeeman transition energy $2Z = g_n\beta_n B$.

In the present work, we are concerned with the various magnetic transitions induced when the excitation magnetic field $\mathbf{B}_1$ is perpendicular to the Zeeman field $\mathbf{B}$. We do wish to mention that parallel-field magnetic resonance ($\mathbf{B}_1 \parallel \mathbf{B}$) too occurs [13], with interesting aspects even for isotropic systems, but this topic will not be covered herein.

3. Conclusions

We have investigated in some detail the theory underlying the energy-level schemes of chemical entities XL_n having equivalent ligands, and have clarified the nature of certain effects found in their magnetic-resonance spectra, which cause complications spoiling the commonly expected simplicity of such spectra. Exact solutions for the spin-hamiltonian energies, as well as expressions for the EPR transition energies and spectral relative intensities, have been given herein for molecules XL_3. This includes discussion of the unusual set of EPR lines caused by hyperfine-induced mixing of the spin states. Some subtle intrinsic effects of the unresolved splitting of the middle lines, comparing X-band spectra, are demonstrated, as are non-standard effects observable to low magnetic fields and at low excitation frequencies. It is expected that some of the phenomena described herein will be seen in the spectral lines coming from outer space, i.e., derived from the burgeoning field of astro-EPR.

Acknowledgments

We thank the Natural Sciences and Engineering Research Council (NSERC) of Canada for some support. One of us (S.M.N.) wishes to acknowledge his indebtedness to Prof. Y. Pan for postdoctoral support.

Appendix A. The spin-hamiltonian and its solution for species XL_3

The energy matrix built on all $(2S+1)(2I+1)^n$ spin states is a 16×16 matrix. This matrix can be factorized into two 1×1, two 4×4 and one 6×6 matrices.

For convenience, let us define electron and nucleus Zeeman-energy symbols $Y \equiv g\beta_e B/2$ and $Z \equiv g_n\beta_n B/2$. The labels on the energies E_j and state kets ϕ_j are $j = 1, \ldots, 16$ in order of decreasing energies as they occur in the highest B-field region, taking Y and Z to be positive, and assuming $Y \gg Z$. The labels then are independent of A.

We define four angles $\xi(g,g_n,A,B) = \delta_1, \delta_2, \eta_1, \eta_2$ useful in writing the ket mixing coefficients (see below). They may be obtained by obtaining the various sets of eigenkets from the four distinct non-diagonal 2×2 secular submatrices given below. The sign of each $\cos\xi \sin\xi$ is relevant but not the signs of the individual trig functions, since the signs of the combination kets have no physical meaning, and the transition intensities go as the squares of the intensity factors listed in Tables 1 and 2 (Columns 4). The angles obey the relations:

$$\tan 2\delta_1 = (\sqrt{3}A/2)/(Y + Z + A/2),$$
$$\tan 2\delta_2 = (\sqrt{3}A/2)/(Y + Z - -A/2),$$
$$\tan 2\eta_1 = A/(Y + Z),$$
$$\tan 2\eta_2 = (A/2)/(Y + Z).$$

Note that $\tan(2\eta_1)$ and $\tan(2\eta_2)$ have the same sign as A, for $Y + Z > 0$.

The first two matrices, 1×1, give two states, with total spin projections (F_z alias M_F), energies and eigenkets:

$$F_z = +2,$$
$$E_8 = 3A/4 + Y - 3Z,$$
$$\phi_8 = |2, +2, {}^{+3/2}\mathrm{A}_1\rangle = |+, {}^{+3/2}\mathrm{A}_1\rangle = |+, + + +\rangle.$$

$$F_z = -2,$$
$$E_9 = 3A/4 - Y + 3Z,$$
$$\phi_9 = |2, -2, {}^{-3/2}\mathrm{A}_1\rangle = |-, {}^{-3/2}\mathrm{A}_1\rangle = |-, - - -\rangle.$$

The 4×4 matrix for states with $F_z = +1$ is

	$\vert -, {}^{+3/2}\mathrm{A}_1\rangle$	$\vert +, {}^{+1/2}\mathrm{A}_1\rangle$	$\vert +, {}^{+1/2}\mathrm{E}_1 > \rangle$	$\vert +, {}^{+1/2}\mathrm{E}_2\rangle$
$\vert -, {}^{+3/2}\mathrm{A}_1\rangle$	$-3A/4 - Y - 3Z$	$\sqrt{3}A/2$	0	0
$\vert +, {}^{+1/2}\mathrm{A}_1\rangle$	$\sqrt{3}A/2$	$A/4 + Y - Z$	0	0
$\vert +, {}^{+1/2}\mathrm{E}_1\rangle$	0	0	$A/4 + Y - Z$	0
$\vert +, {}^{+1/2}\mathrm{E}_2\rangle$	0	0	0	$A/4 + Y - Z$

The 4×4 matrix for states with $F_z = -1$ is

	$\vert +, {}^{-3/2}\mathrm{A}_1\rangle$	$\vert -, {}^{-1/2}\mathrm{A}_1\rangle$	$\vert -, {}^{-1/2}\mathrm{E}_1\rangle$	$\vert -, {}^{-1/2}\mathrm{E}_2\rangle$
$\vert +, {}^{-3/2}\mathrm{A}_1\rangle$	$-3A/4 + Y + 3Z$	$\sqrt{3}A/2$	0	0
$\vert -, {}^{-1/2}\mathrm{A}_1\rangle$	$\sqrt{3}A/2$	$A/4 - Y + Z$	0	0
$\vert -, {}^{-1/2}\mathrm{E}_1\rangle$	0	0	$A/4 - Y + Z$	0
$\vert -, {}^{-1/2}\mathrm{E}_2\rangle$	0	0	0	$A/4 - Y + Z$

The 6×6 matrix for states with $F_z = 0$ is

	$\vert -, {}^{+1/2}\mathrm{A}_1\rangle$	$\vert +, {}^{-1/2}\mathrm{A}_1\rangle$	$\vert -, {}^{+1/2}\mathrm{E}_1\rangle$	$\vert +, {}^{-1/2}\mathrm{E}_1\rangle$	$\vert -, {}^{+1/2}\mathrm{E}_2\rangle$	$\vert +, {}^{-1/2}\mathrm{E}_2\rangle$
$\vert -, {}^{+1/2}\mathrm{A}_1\rangle$	$-A/4 - Y - Z$	A	0	0	0	0
$\vert +, {}^{-1/2}\mathrm{A}_1\rangle$	A	$-A/4 + Y + Z$	0	0	0	0
$\vert -, {}^{+1/2}\mathrm{E}_1\rangle$	0	0	$-A/4 - Y - Z$	$-A/2$	0	0
$\vert +, {}^{-1/2}\mathrm{E}_1\rangle$	0	0	$-A/2$	$-A/4 + Y + Z$	0	0
$\vert -, {}^{+1/2}\mathrm{E}_2\rangle$	0	0	0	0	$-A/4 - Y - Z$	$-A/2$
$\vert +, {}^{-1/2}\mathrm{E}_2\rangle$	0	0	0	0	$-A/2$	$-A/4 + Y + Z$

The 3rd matrix gives four solutions (1 pair degenerate) for states with $F_z = +1$:

$$E_5 = -A/4 - 2Z + \{(Y + Z + A/2)^2 + (3/4)A^2\}^{1/2},$$
$$= -A/4 - 2Z + (Y + Z + A/2)/\cos(2\delta_1),$$
$$\phi_5 = |2, +1, \mathrm{A}_1^{\mathrm{i}} >= \sin\delta_1|-, {}^{+3/2}\mathrm{A}_1\rangle + \cos\delta_1|+, {}^{+1/2}\mathrm{A}_1\rangle.$$

$$E_6 = E_7 = A/4 + Y - Z,$$
$$\phi_6 = |1, +1, {}^{+1/2}\mathrm{E}_1\rangle$$
$$= (1/\sqrt{6})(2|+, - + +\rangle - |+, + - +\rangle - |+, + + -\rangle),$$
$$\phi_7 = |1, +1, {}^{+1/2}\mathrm{E}_2\rangle = (1/\sqrt{2})(|+, - + +\rangle - |+, + + -\rangle).$$

$$E_{16} = -A/4 - 2Z - \{(Y + Z + A/2)^2 + (3/4)A^2\}^{1/2}$$
$$= -A/4 - 2Z - (Y + Z + A/2)/\cos(2\delta_1),$$
$$\phi_{16} = |1, +1, \mathrm{A}_1^{\mathrm{ii}} >= \cos\delta_1|-, {}^{+3/2}\mathrm{A}_1\rangle - -\sin\delta_1|+, {}^{+1/2}\mathrm{A}_1\rangle.$$

Solution of the 4th matrix gives 4 energy states (1 pair degenerate) for states with $F_z = -1$:

$$E_1 = -A/4 + 2Z + \{(Y + Z - A/2)^2 + (3/4)A^2\}^{1/2},$$
$$= -A/4 + 2Z + (Y + Z - A/2)/\cos(2\delta_2),$$
$$\phi_1 = |2, -1, \mathrm{A}_1^{\mathrm{iii}}\rangle = \cos\delta_2|+, {}^{-3/2}\mathrm{A}_1\rangle + \sin\delta_2|-, {}^{-1/2}\mathrm{A}_1\rangle.$$

$$E_{10} = E_{11} = A/4 - Y + Z,$$
$$\phi_{10} = |1, -1, {}^{-1/2}\mathrm{E}_1\rangle = |-, {}^{-1/2}\mathrm{E}_1\rangle$$
$$= (1/\sqrt{6})(2|-, + - -\rangle - |-, - + -\rangle - |-, - - +\rangle),$$
$$\phi_{11} = |1, -1, {}^{-1/2}\mathrm{E}_2\rangle = |-, {}^{-1/2}\mathrm{E}_2\rangle$$
$$= (1/\sqrt{2})(|-, - + -\rangle - |-, - - +\rangle).$$

$$E_{12} = -A/4 + 2Z - \{(Y + Z - A/2)^2 + (3/4)A^2\}^{1/2}$$
$$= -A/4 + 2Z - (Y + Z - A/2)/\cos(2\delta_2),$$
$$\phi_{12} = |1, -1, \mathrm{A}_1^{\mathrm{iv}}\rangle = \cos\delta_2|-, {}^{-1/2}\mathrm{A}_1\rangle - \sin\delta_2|+, {}^{-3/2}\mathrm{A}_1\rangle.$$

The 5th matrix (6×6) gives 6 states (2 pairs degenerate) with $F_z = 0$:

$$E_2 = -A/4 + \{(Y + Z)^2 + A^2\}^{1/2}$$
$$= -A/4 + (Y + Z)/\cos(2\eta_1),$$
$$\phi_2 = |2, 0, \mathrm{A}_1^{\mathrm{v}}\rangle = \cos\eta_1|+, {}^{-1/2}\mathrm{A}_1\rangle + \sin\eta_1|-, {}^{+1/2}\mathrm{A}_1\rangle\}.$$
$$E_3 = E_4 = -A/4 + \{(Y + Z)^2 + (A/2)^2\}^{1/2}$$
$$= -A/4 + (Y + Z)/\cos(2\eta_2),$$
$$\phi_3 = |1, 0, \mathrm{E}_1^{\mathrm{i}}\rangle = \cos\eta_2|+, {}^{-1/2}\mathrm{E}_1\rangle - \sin\eta_2|-, {}^{+1/2}\mathrm{E}_1\rangle,$$
$$\phi_4 = |1, 0, \mathrm{E}_2^{\mathrm{i}}\rangle = \cos\eta_2|+, {}^{-1/2}\mathrm{E}_2\rangle - \sin\eta_2|-, {}^{+1/2}\mathrm{E}_2\rangle.$$

$$E_{13} = E_{14} = -A/4 - \{(Y+Z)^2 + (A/2)^2\}^{1/2}$$
$$= -A/4 - (Y+Z)/\cos(2\eta_2),$$
$$\phi_{13} = |0,0,\mathrm{E}_1^{\mathrm{ii}}\rangle = \sin\eta_2|+,{}^{-1/2}\mathrm{E}_1\rangle + \cos\eta_2|-,{}^{+1/2}\mathrm{E}_1\rangle,$$
$$\phi_{14} = |0,0,\mathrm{E}_2^{\mathrm{ii}}\rangle = \sin\eta_2|+,{}^{-1/2}\mathrm{E}_2\rangle + \cos\eta_2|-,{}^{+1/2}\mathrm{E}_2\rangle.$$
$$E_{15} = -A/4 - \{(Y+Z)^2 + A^2\}^{1/2}$$
$$= -A/4 - (Y+Z)/\cos(2\eta_1),$$
$$\phi_{15} = |1,0,\mathrm{A}_1^{\mathrm{vi}}\rangle = \cos\eta_1|-,{}^{+1/2}\mathrm{A}_1\rangle - \sin\eta_1|+,{}^{-1/2}\mathrm{A}_1\rangle.$$

Note that various of the nuclear-spin kets used above were defined in the above test.

Appendix B. Cautionary note on ordering

Care must be taken in labeling the spin states and the transitions, to be arranged in some order. First of all, one must state whether one is dealing with the manifold of energy states (Case $\mathrm{E_a}$) or with a set of transitions (Case $\mathrm{E_b}$).

In the Case $\mathrm{E_a}$, one usually refers herein to the order of energies occurring in (or near) the high magnetic-field limit (see Fig. 1b, for system $\mathrm{XL_3}$). Let us utilize, instead of the analytic general notation used in the text (see Appendix A), the more usual notation

$$E(M_S, M_I) = g\beta_e B M_S + (AM_S - g_n\beta_n B)M_I + \cdots \quad \text{(B-1)}$$

and

$$h\nu = \Delta E_{\mathrm{EPR}}(M_I) \quad \text{(B-2a)}$$
$$= g\beta_e B + AM_I + \cdots. \quad \text{(B-2b)}$$

for primary EPR transitions.

Depending on the relative sign(s) of parameters A and g_n, the second right-hand term (see Eq. (B-2a)) may go through zero as a series of A values is encountered, for some B-value region (say, for EPR X-band), due to the cancellation of the hyperfine and nuclear Zeeman terms. At that point, one subset of energy levels will reverse its order, and hence their labels; it may be evident from Fig. 2 (system $\mathrm{XL_3}$, where $2M_I = -3, -1, +1, +3$) that this can happen for the upper octet, switching from $1, 2, \cdots, 8$ to $8, 7, \cdots, 1$. With X-band EPR (say, 9.1 GHz and $g = g_e$), the resonant field is ca. 325 mT, and hence $A/(g_e\beta_e)$ for protons is ca. 0.99 mT at this level crossing. Of course, at sufficiently high B fields, the nuclear-Zeeman term will dominate in Eq. (B-1).

With regard to the energy-level crossings (i.e., level reordering) evident in Fig. 1a, it can easily be shown (taking Z to be negligible), that these occur as follows:

1) Single crossing @ $B \approx (1/2)|A|/(\mathrm{g_e}\beta_e)$
2) Double crossing @ $B \approx (3/4)|A|/(\mathrm{g_e}\beta_e)$
3) Triple crossing @ $B \approx (3/2)|A|/(\mathrm{g_e}\beta_e)$

and (not shown in Fig. 1a), with Z included, various crossings:

4) Grand crossing region @ $B \approx M_S A/(\mathrm{g_n}\beta_n)$ (See Eq. (B-1)).

Here $M_S = +1/2$ when $A/g_n > 0$. For protons and $A/(g_e\beta_e) = 0.50$ mT, this occurs near 165 mT. There are 13 crossings within the region 163.54–165.05 mT. In terms of the highest-field labels *1*, *2*, {*3*,*4*}, *5*, {*6*,*7*}, *8* for the upper octet where *1* denotes the highest energy, the scheme at 2 mT (Fig. 1a) is *8*, *1*, {*6*,*7*}, *2*, {*3*,*4*}, *5* and then, below these, the set *9*, {*10*,*11*}, *12*, {*13*,*14*}, *15*, *16*.

Note that, at zero B field, when $A > 0$, the eigenkets ϕ_j occur in the order (see Fig. 1a; $A/(g_e\beta_e) = 0.50$ mT): $j = \{8,1,2,5,9\}$, $\{\{6,7\}, \{3,4\}, \{10,11\}\}$, $\{13,14\}$ and $\{12,15,16\}$, beginning with the highest energy. In the limit $B \to \infty$, one will attain *1*, {*2*,*3*,*4*}, {*5*,*6*,*7*}, *8* situated above the set *9*, {*10*,*11*,*12*}, {*13*,*14*,*15*}, *16*.

It is obvious that if one is labeling resonant magnetic fields B_i (say in fixed-frequency EPR), their order will be just opposite to that of the corresponding frequencies ν_i (see Eq. (B-2a)) in fixed-field EPR.

Equal care must be taken when labeling spectral lines by those who adopt the pernicious habit of using 'artificial' g values to do so.

References

[1] S.M. Nokhrin, J.A. Weil, D.F. Howarth, Magnetic resonance in systems with equivalent spin-1/2 nuclides. Part 1, J. Magn. Reson. 174 (2005) 209–218.
[2] G. Baym, Lectures on Quantum Mechanics, W.A. Benjamin, New York, NY, USA, 1969.
[3] J.A. Weil, J.R. Bolton, Electron Paramagnetic Resonance – Elementary Theory and Practical Applications, 2nd edition., John Wiley & Sons, New York, NY, USA, 2007.
[4] J.A. Weil, Comments on second-order spin-hamiltonian energies, J. Magn. Reson. 18 (1975) 113–116.
[5] J.A. Pople, W.G. Schneider, H.J. Bernstein, High-resolution Nuclear Magnetic Resonance, McGraw-Hill, New York, NY, USA, 1959.
[6] P.L. Corio, Structure of High-resolution NMR Spectra, Academic Press, New York, NY, USA, 1966.
[7] H.M. McConnell, A.D. McLean, C.A. Reilly, Analysis of spin–spin multiplets in nuclear magnetic resonance spectra, J. Chem. Phys. 23 (6) (1955) 1152–1159.
[8] R.W. Fessenden, Second-order splittings in the ESR spectra of organic radicals, J. Chem. Phys. 37 (4) (1962) 747–750.
[9] M. Hamermesh, Group Theory and its Applications to Physical Problems, Addison-Wesley, Reading, MA, USA, 1962.
[10] L.D. Landau, E.M. Lifshitz, Quantum Mechanics – Non-relativistic Theory, Vol. 3, Addison-Wesley, Reading, MA, USA, 1958.
[11] M.J. Mombourquette, J.A. Weil, Computer Program EPR–NMR, Department of Chemistry, University of Saskatchewan, 110 Science Place, Saskatoon, SK, S7N 5C9, Canada 1995 (Version 6.5.3, 2007).
[12] S.W. Charles, P.H.H. Fisher, C.A. McDowell, Electron spin resonance study of the photolytic decomposition of CF_3I in inert matrices between 4.2 K and 35 K, Chem. Phys. Lett. 1 (1967) 451–454.
[13] J.A. Weil, The hydrogen atom revisited: parallel-field magnetic resonance, Concepts Magn. Reson. 28A (5) (2006) 331–336.